

Fivefold Symmetry in Superlattices of Monolayer-Protected Gold Nanoparticles

Hiroshi Yao,* Takayuki Minami, Akihiko Hori, Masaya Koma, and Keisaku Kimura

Graduate School of Material Science, University of Hyogo, 3-2-1 Koto, Kamigori-cho, Ako-gun, Hyogo 678-1297, Japan

Received: June 1, 2006; In Final Form: June 23, 2006

Three-dimensional (3D) superlattices of gold nanoparticles were prepared at an air/solution interface. The surface of the gold nanoparticles used is protected by *N*-acetylglutathione (NAG). Morphological studies revealed that the superlattices formed fivefold symmetric structures such as pentagonal rod, decahedron, and icosahedron, which were probably developed by multiple twinning. Moreover, high-resolution surface images of the superlattices in fivefold symmetry showed excellent ordered arrangements of nanoparticles with both close-packed and non-close-packed structures.

Introduction

Metal nanoparticles have a variety of interesting spectroscopic, electronic, and chemical properties that arise from their small sizes and high surface/volume ratios.¹ In recent years, particular emphasis has been placed on the control of shape because in many cases it allows one to fine-tune the properties with a greater versatility than can be achieved otherwise.^{2,3} The particle shapes are closely related to the crystallographic surfaces that enclose the particles. In face-centered cubic (fcc) metal particles, the {111} and {100} surfaces are different not only in the surface atom densities but also in surface energies, so that single-crystalline silver or gold nanoparticles with sizes smaller than ~10 nm show intriguing particle shapes such as truncated octahedra or cuboctahedra.⁴ In addition, twinned metal particles are found.⁴ Twinning is the result of two subgrains sharing a common crystallographic plane, and thus, multiple twinning on alternate coplanar planes produces cyclic twinned polyhedra (decahedra and icosahedra) where the twinned tetrahedral subunits are arranged around fivefold axes.⁵ In small nanoparticles, they can reduce their surface energy by adopting a fivefold symmetric structure, and this may overcome the internal strain caused by some lattice distortion in the arrangements.⁵

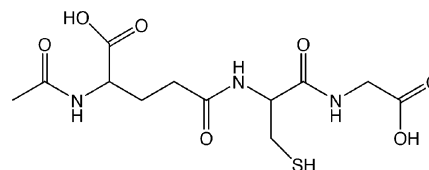
Meanwhile, construction of ordered assemblies or superlattices on nanoscale dimensions is of key interest not only in electronics applications but also in fundamental nanoscience.^{6,7} Metal nanoparticles, which will be considered as “artificial atoms”, are ideal building blocks for two- (2D) and three-dimensional (3D) superlattice structures. Preparation of such ordered assemblies often requires surface passivation of the “building blocks” to protect against modifications of their properties by their environment, as well as to inhibit their property to sinter. The organic surface protection of nanoparticles then enables them to self-assemble into their superlattices, so that controlling the chemical functionality of the organic monolayer allows the collective properties of the nanoparticle superlattices to be engineered.⁶

Unlike the most successful approaches that utilize hydrophobic alkanethiols as a surface modifier in gold nanoparticles,⁷ we have developed the syntheses of carboxylate-protected water-soluble gold nanoparticles.^{8,9} Application of such hydrophilic nanoparticles is one of the new fields for the construction of 3D superlattices not by weak van der Waals interaction but by strong hydrogen-bonding and/or electrostatic interactions.⁹ Actually, we have succeeded in preparing single-crystalline 3D superlattices consisting of mercaptosuccinic acid-protected gold nanoparticles. The superlattices form at an air/water interface under highly acidic conditions (pH < 2), and they are connected through hydrogen bonds among the surface carboxylic acids.^{10,11}

In the present study, we construct 3D superlattices consisting of *N*-acetylglutathione (NAG)-protected gold nanoparticles. Glutathione (γ -Glu-Cys-Gly) is one of the most favorable surface protecting agents that contain both carboxyl and amino groups,⁸ so that it can be a zwitterion under near-neutral pH conditions. The *N*-acetylation of the amino group in glutathione inhibits to produce the zwitterion, and the strategy for preparing nanoparticle superlattices via hydrogen bonding among carboxylic acid molecules can be applied. During the superlattice syntheses, we found for the first time that fivefold symmetric (pentagonal, decahedral, and icosahedral) superstructures could be built from NAG-protected gold nanoparticles. We here report the structural nature in the fivefold symmetric superlattices.

Experimental Section

Preparation of *N*-acetylglutathione (NAG), that is, *N*-acetylation of glutathione, was carried out according to the literature procedure.¹² The chemical structure is shown in Scheme 1. The synthesis of NAG-protected gold nanoparticles involves the

SCHEME 1: *N*-Acetylglutathione (NAG)

* Corresponding author. Phone: +81-791-58-0160. Fax: +81-791-58-0161. E-mail: yao@sci.u-hyogo.ac.jp.

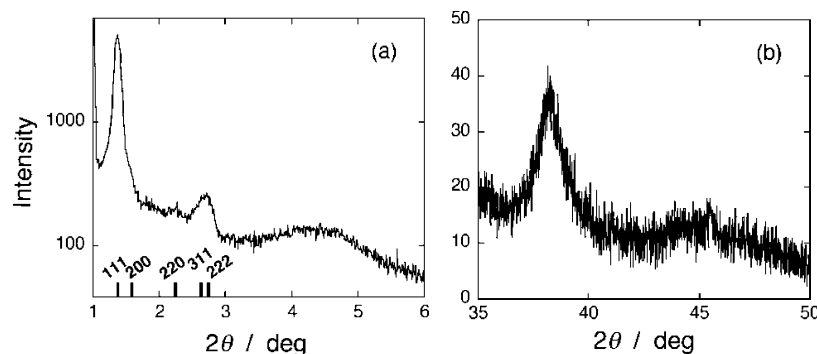


Figure 1. (a) Small-angle XRD profile of the superlattice sample, suggesting a nanoscale periodicity caused by the formation of ordered arrays of gold nanoparticles. (b) Wide-angle XRD profile of the superlattice sample.

preparation of an aqueous gold–NAG complex followed by the reduction of the metal ions with sodium borohydride (NaBH_4) under a fixed NAG/Au molar ratio. Briefly, 0.5 mmol of HAuCl_4 dissolved as 2% (w/v) aqueous solution was first mixed with 1.0 mmol of NAG in 100 mL of methanol to give a transparent solution. A freshly prepared ice-cooled 0.2 M aqueous NaBH_4 solution (25 mL) was then added at a rate of 2.5 mL/min under vigorous stirring. The solution turned dark-brown immediately. After further stirring of 1.5 h, ethanol/acetic acid (100/1) was added to produce precipitate. The precipitate was washed with the ethanol/acetic acid (100/1) solution repeatedly through a redispersion–centrifugation process to remove undesirable impurities. Finally, the precipitate dissolved in water was freeze-dried.

We have found that carboxylate-protected gold nanoparticles self-assemble into superlattices or ordered arrays at an air/aqueous solution interface by adding a concentrated hydrochloric acid (HCl),¹¹ so the preparation of 3D nanoparticle superlattices was conducted as follows: The as-prepared NAG-protected gold nanoparticle powder (6.0 mg) was dispersed in 0.05 M HCl solution (2.0 mL) to form suspensions and stored in a closed vessel for about 3 weeks. Crystallization or superlattice formation took place at the air/solution interface, showing mirrorlike light reflection due to the formation of gold nanoparticle superlattices.

Results and Discussion

The as-prepared sample analyses reveal the chemical properties of NAG-protected gold nanoparticles. On the basis of FT-IR measurements, we obtained the following results on the surface chemistry of the nanoparticles (see the Supporting Information): NAG molecules anchor on the gold nanoparticle surface through the sulfur atom in the SH group (as revealed by the disappearance of the S–H stretch mode at $\sim 2570\text{ cm}^{-1}$). The surface modifier on nanoparticle surfaces contains the bands of amido-I ($\text{C}=\text{O}$ stretch in NHCO ; 1640 cm^{-1}) and amido-II ($\text{N}-\text{H}$ bending in NHCO ; 1540 cm^{-1}) along with those for the stretch modes of COO^- (1600 and 1395 cm^{-1}). The powder X-ray diffraction (XRD) profile exhibited broad crystalline peaks of gold, and the nanoparticle core diameter, calculated from the Scherrer equation,⁸ was 1.4 nm using the half width of the intense (111) reflection at $2\theta = 38.2^\circ$ (see the Supporting Information).¹³

The NAG-protected gold nanoparticles self-assemble into ordered arrays or superlattices at an air/aqueous solution interface by adding a concentrated hydrochloric acid of 0.05–0.1 M.¹¹ Storage of the solution in a closed vessel for about 3 weeks provided the superlattices, and their morphology and packing structure were characterized by XRD analyses and field emission scanning electron microscopy (FE-SEM) observations

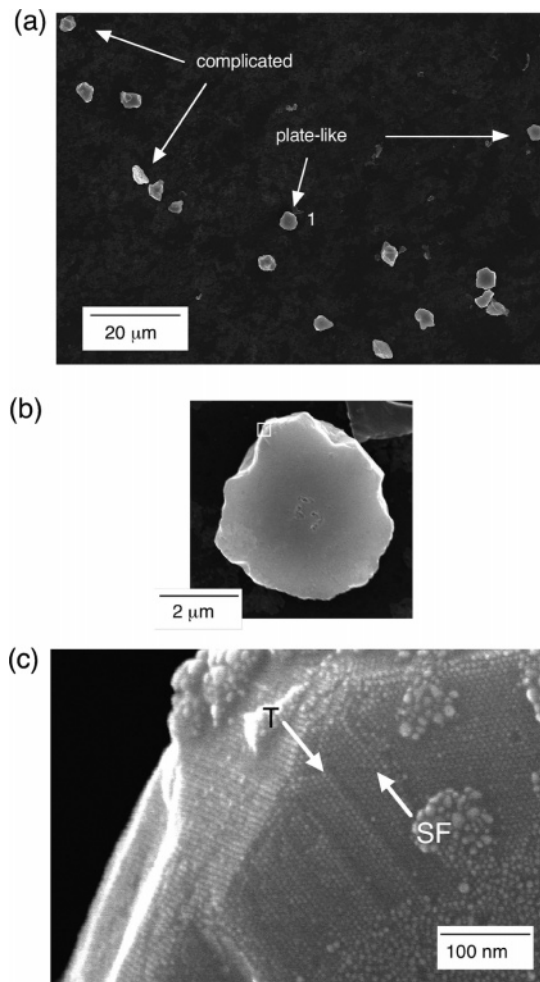


Figure 2. (a) FE-SEM images of superlattices of NAG-protected gold nanoparticles on a Si substrate. The superlattices show a variety of morphologies having well-defined facets. (b and c) Magnified images of the superlattice marked with 1. The image clarified the hexagonal close-packed arrangement of nanoparticles. In part c, examples of the twin and stacking fault are marked with “T” and “SF”, respectively.

(Hitachi S-4800). The superlattice samples were placed onto a Si substrate. The small-angle XRD profile shows several peaks (Figure 1a), suggesting nanometer-scale periodicity caused by the formation of superlattices of NAG-protected gold nanoparticles. The constituent gold nanoparticles were stacked in a pattern of fcc rather than hcp (hexagonal close-packing) with a lattice constant of 11.1 nm (or center-to-center distance of 7.86 nm), as determined by the simulation of the peak positions. The second-order peak was observed only for the 111 reflection, indicating the presence of considerable stacking defects in

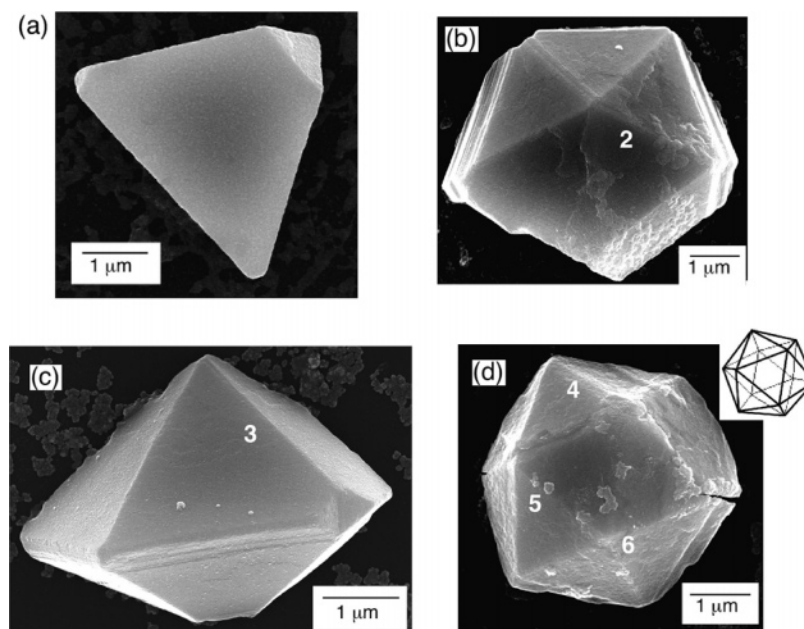


Figure 3. Superlattices of (a) tetrahedral, (b) pentagonal rodlike, (c) decahedral, and (d) icosahedral shapes. The inset in part d shows the geometrical model of an icosahedron in the same orientation.

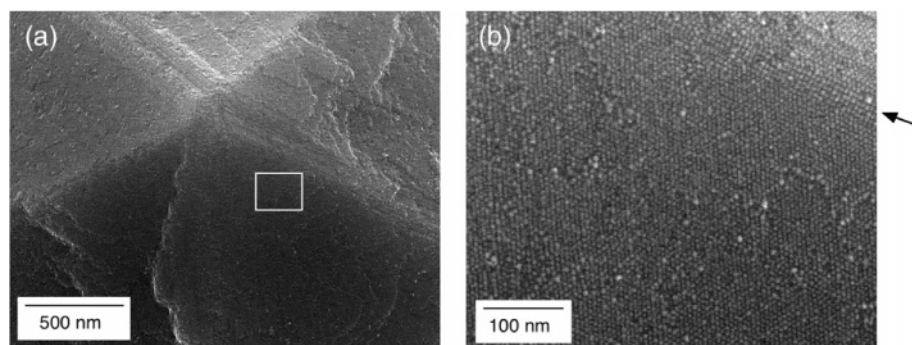


Figure 4. Magnified FE-SEM images at the vicinity of the edge region marked with **2** in Figure 3b. The arrow indicates the truncated common edge.

superlattices. Note that the lattice constant obtained from the small-angle XRD is larger than that estimated from the average diameter of the as-prepared gold nanoparticles. The increase in core size of the constituent gold nanoparticles was confirmed by the wide-angle XRD pattern (Figure 1b), giving an average diameter of ~ 6.8 nm (from the Scherrer formula). A transmission electron microscopy (TEM) micrograph of particles at the vicinity of the superlattices also revealed an increase in the core size of gold nanoparticles (average diameter = 6.3 nm, close to the size determined by XRD; see the Supporting Information). On the basis of these size estimations, the surface-to-surface distance between adjacent nanoparticles in the superlattices is determined to be 1.1–1.5 nm. By comparing this distance with the length of an NAG molecule (~ 1.0 nm), the surface protecting agents are partly interdigitated with each other. Although the mechanism for the size increase is unclear at present, the growth of nanoparticles would take place during the superlattice formation in consideration of the following studies that support our observation:¹⁴ The study on the stability of size-selected glutathione-protected gold nanoclusters shows that some of them were unstable against decomposition whereas thermodynamically stable nanoclusters were enhanced.¹⁵ In addition, the other study on the formation of monodisperse nanoparticles indicates that digestive-like ripening, wherein a polydisperse nanoparticles is digested during heating of the

solvent, could induce a change of size and distribution of the monolayer-protected gold particles.¹⁶

FE-SEM observations elucidate a variety of shapes in the 3D nanoparticle superlattices having well-defined or multiple facets, where many of them had platelike or complicated morphologies (Figure 2a). Magnified images of the platelike superlattice marked with **1** (Figure 2b and c) clarified the hexagonal close-packed arrangement of nanoparticles with a core size of about 6 nm. In addition, the lattice image observed at the side facets confirmed the 3D ordered arrangement of the nanoparticles. However, a further observation of the surface image reveals the presence of twin planes and stacking faults. Examples of the twin and stacking fault are marked with “T” and “SF” in Figure 2c, respectively. Hence, it is expected that 3D superlattices of NAG-protected gold nanoparticles can be easily twinned, and the observed complicated morphology having clear facets would result from the twinned structures. In crystallography, the crystal habit depends on the internal structure and the growth conditions as well as on the kinetics of growth.^{4a} If the superlattices are formed in thermodynamic equilibrium, their shape results from minimizing the surface energy. On the contrary, the observed morphologies of the superlattice suggest that its formation is dominated by the kinetics of growth that can promote crystal growth through stacking faults and twins.

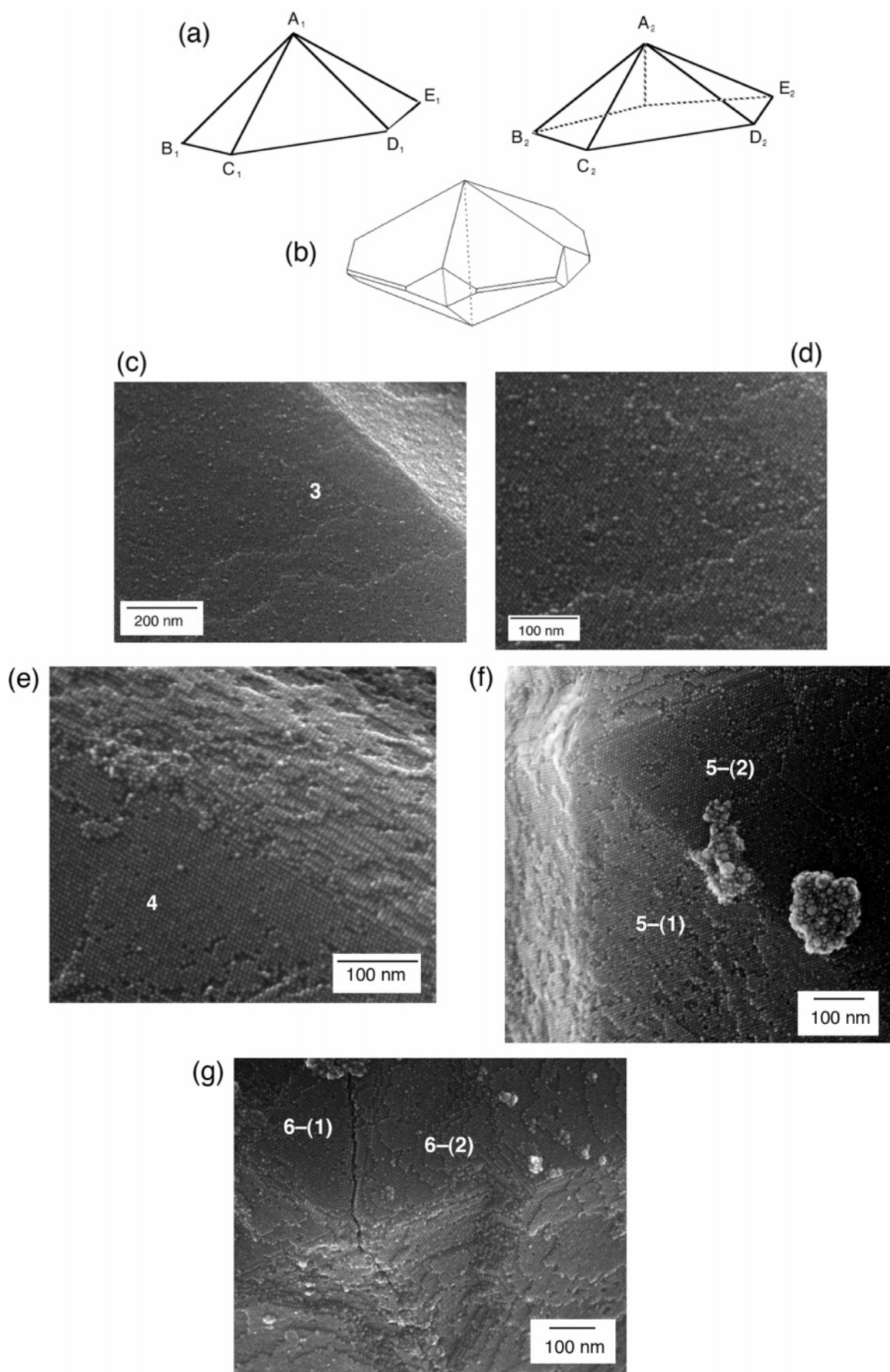


Figure 5. (a) Contour of the upper half of the superlattice in Figure 3c (left, re-entrant corners are excluded) and the ideal pentagonal model (right) in the same orientation. (b) Marks decahedron having re-entrant corners. (c and d) Magnified surface image around the region marked with **3** in Figure 3c. (e–g) Magnified surface images around the regions marked with **4–6** in Figure 3d. The nanoparticle arrangements in the regions of **4** and **5-(1)** differ from those of **5-(2)**, **6-(1)**, and **6-(2)** of $\{111\}$ -like planes.

We should also mention that different shapes of superlattices were observed: tetrahedron, pentagonal rod, decahedron, and icosahedron shown in parts a–d of Figure 3, respectively. Note that, in Figure 3c, we cannot see the opposite side of the structure; however, for both symmetry reason and geometrical coincidence of the upper half of the superlattice (Figure 5a, left; re-entrant corners were excluded) with that of the ideal pentagonal model (Figure 5a, right) in the same orientation, this structure should be decahedral. The strong emphasis is placed on the first observation of *fivefold symmetry* in the nanoparticle superlattices (Figure 3b–d). These shapes would come from multiple twinning.⁵ In the pentagonal rodlike superlattice, the habits were somewhat modified; that is, new faces were developed instead of vertices or edges: (i) Re-entrant corners (or notches) can be seen. The growth of the notches implies the development of star-shaped superlattices. (ii) The common edges in the structure are truncated to form other faces. Figure 4 shows the magnified FE-SEM images at the vicinity of the edge region marked with 2 in Figure 3b. The triangular face is the close-packed {111}-like plane, whereas the truncated face shows a tetragonal {112}-like plane (see the arrow in Figure 4b).⁵ The facets that appear are generally a high-energy surface compared to the close-packed plane due to high-index crystallography planes, but the edge truncation is very effective for lowering the surface/volume ratio.

It is known that the two most typical fivefold twinning are decahedron and icosahedron. A decahedron is assembled from five tetrahedral subunits sharing an edge. An icosahedron is assembled using 20 tetrahedral subunits via sharing an apex.⁵ Intrinsically, tetrahedral subunits in fcc cannot form a complete space-filling structure, so that there remains angular misfit yielding internal strain. The strain is relaxed by a reduction of surface energy up to a certain size above which transformation to single-crystalline particles is expected. Hence, a fivefold twinned particle is commonly bounded by the lowest-energy triangular facets. In regular decahedra, they have a large surface/volume ratio, which can be lowered by truncating the edges around the common basis, thus obtaining the Ino decahedra with five {100}-like facets.¹⁷ An even better structure is the Marks decahedra, obtained by introducing re-entrances that separate the {100}-like facets.¹⁸ In Figure 3c, the observed re-entrant corners are well characterized by a typical Marks decahedron whose schematic drawing is shown in Figure 5b.

On the other hand, an icosahedral particle normally contains a larger strain inside due to the distortion of the intershell and intrashell distances, so that this form could be present only at small sizes in metal nanoparticles. For example, a size limit of 27.35 nm has been obtained in icosahedral silver nanoparticles, whereas a size limit of 273.3 nm has been obtained in decahedra.^{17,19} Note that the total number of silver atoms in an icosahedral nanoparticle of ~27 nm can be approximately estimated to be $(4-5) \times 10^5$, corresponding to 40–50 shells.^{20a} Surprisingly, in Figure 3d, $(1-2) \times 10^8$ nanoparticles are included in the superlattice of ~4 μm assuming that they are made of spheres of 7.9 nm in diameter (i.e., center-to-center distance between adjacent nanoparticles), which correspond to 300–400 shells.^{20b} This is probably due to the fact that a large relaxation of the internal strain caused by the size nonuniformity (or flexibility) of the constituent nanoparticles makes the icosahedral structure much more stable. However, the strain remaining in the structure could collapse the regular shape when handling the superlattice samples distributed at the air/solution interface (see one edge in Figure 3d).

High-resolution images at the boundary surfaces of decahedral and icosahedral superlattices provide interesting characteristics on the arrangements of nanoparticles. Figure 5c–g shows the magnified surface images around the regions marked with 3–6 in Figure 3. For example, faces referred to as 5-(2), 6-(1), and 6-(2) are in the close-packed hexagonal arrangement of nanoparticles ({111}-like planes), whereas those referred to as 3, 4, and 5-(1) are in distorted tetragonal (non-close-packed) arrangements that are ascribed to different index planes.²¹ The results indicate that these surface planes having different packing structures are energetically similar to each other. Since the individual NAG-protected gold nanoparticles are composed of both nanoscaled metallic-core and molecular-shell parts, multiple interactions among the nanoparticle units that involve van der Waals and hydrogen-bonding interactions would contribute to this phenomenon. Further investigations are under way to explore the structural properties in more detail.

Conclusion

In conclusion, 3D gold nanoparticle superlattices were produced at an air/solution interface under highly acidic conditions. The surface of the gold nanoparticles used was protected by *N*-acetylglutathione (NAG) that can bind the constituent nanoparticles via hydrogen bonds.¹¹ Morphological studies by FE-SEM revealed that the superlattices formed fivefold symmetric structures such as pentagonal rod, decahedron, and icosahedron, which were probably developed by multiple twinning. High-resolution surface images of the superlattices in fivefold symmetry showed excellent ordered arrangements of nanoparticles with both close-packed and non-close-packed structures. The field of fivefold twinned structures is a very broad and complicated one ranging from cluster science to surface science, so we believe that our findings will give a new development of this fascinating subject in nanoscience.

Acknowledgment. The present work was financially supported by Grant-in-Aids for Scientific Research from MEXT (S: 16101003), Scientific Research in Priority Areas: Application of Molecular Spins (15087210), and Grant from Kawanishi Memorial Shinmeiwa Education Foundation.

Supporting Information Available: The FT-IR spectrum and the XRD pattern of the as-prepared NAG-protected gold nanoparticles, TEM image of the size-increased gold nanoparticles, and FE-SEM images of a superlattice representing the effect of the sample surface inclination. This material is available free of charge via the Internet at <http://pubs.acs.org>.

References and Notes

- (1) (a) Daniel, M.-C.; Astruc, D. *Chem. Rev.* **2004**, *104*, 293. (b) Whetten, R. L.; Shafigullin, M. N.; Koury, J. T.; Schaaff, T. G.; Vezmar, I.; Alvarez, M. M.; Wilkinson, A. *Acc. Chem. Res.* **1999**, *32*, 397. (c) Brust, M.; Walker, M.; Bethell, D.; Schiffrin, D. J.; Whyman, R. *J. Chem. Soc., Chem. Commun.* **1994**, 801. (d) Templeton, A. C.; Wuelfing, W. P.; Murray, R. W. *Acc. Chem. Res.* **2000**, *33*, 27.
- (2) Wiley, B.; Sun, Y.; Mayers, B.; Xia, Y. *Chem.—Eur. J.* **2005**, *11*, 454.
- (3) (a) Sosa, I. O.; Noguez, C.; Barrera, R. G. *J. Phys. Chem. B* **2003**, *107*, 6269. (b) Murphy, C. J.; Jana, N. R. *Adv. Mater.* **2002**, *14*, 80.
- (4) (a) Wang, Z. L. *J. Phys. Chem. B* **2000**, *104*, 1153. (b) Marks, L. D. *Rep. Prog. Phys.* **1994**, *57*, 603.
- (5) Hofmeister, H. Fivefold Twinned Nanoparticles. In *Encyclopedia of Nanoscience and Nanotechnology*; Nalwa, H. S., Ed.; American Scientific: Stevenson Ranch, CA, 2004; Vol. 3, p 431.
- (6) Kotov, N. A. *Nanoparticle Assemblies and Superstructures*; Taylor & Francis: Boca Raton, FL, 2006.
- (7) (a) Brust, M.; Kiely, C. J. *Colloids Surf., A* **2002**, *202*, 175. (b) Sampaio, J. F.; Beverly, K. C.; Heath, J. R. *J. Phys. Chem. B* **2001**, *105*,

8797. (c) Zhong, C. J.; Maye, M. M. *Adv. Mater.* **2001**, *13*, 1507. (d) Storhoff, J. J.; Mirkin, C. A. *Chem. Rev.* **1999**, *99*, 1849. (e) Burghard, M.; Philipp, G.; Roth, S.; von Klitzing, S. K.; Pugin, R.; Schmid, G. *Adv. Mater.* **1998**, *10*, 842.

(8) Chen, S.; Kimura, K. *Langmuir* **1999**, *15*, 1075.

(9) (a) Yao, H.; Momozawa, O.; Hamatani, T.; Kimura, K. *Chem. Mater.* **2001**, *13*, 4692. (b) Yao, H.; Momozawa, O.; Hamatani, T.; Kimura, K. *Bull. Chem. Soc. Jpn.* **2000**, *73*, 2675.

(10) Jeffrey, G. A. *An Introduction to Hydrogen Bonding*; Oxford University Press: Oxford, U.K., 1997.

(11) (a) Kimura, K.; Sato, S.; Yao, H. *Chem. Lett.* **2001**, 372. (b) Sato, S.; Yao, H.; Kimura, K. *Physica E* **2003**, *17*, 521. (c) Yao, H.; Kojima, H.; Sato, S.; Kimura, K. *Langmuir* **2004**, *20*, 10317.

(12) Levy, E. J.; Anderson, M. E.; Meister, A. *Anal. Biochem.* **1993**, *214*, 135.

(13) Although we conducted TEM measurements for the as-prepared sample, the particle size and its distribution could not be estimated because the sizes were too small to be exactly analyzed. Hence, the mean particle size was determined by the XRD measurement.

(14) Under acidic conditions, the increase in particle size might involve ligand desorption/readsorption and the growth of metal cores for kinetically stabilized original gold nanoparticles. We believe that the particle growth would be essentially followed by assembling of nanoparticles into a superlattice because, for the superlattice formation, a relatively long period of time (a few weeks) was necessary, implying that the small original

particles are hard to self-assemble with each other. The result is consistent with the fact that large gold nanoparticles organize more readily into superstructures than the small ones due to effective size-dependent van der Waals attractive interactions (Ohara, P. C.; Leff, D. V.; Heath, J. R.; Gelbart, W. M. *Phys. Rev. Lett.* **1995**, *75*, 3466.).

(15) Negishi, Y.; Nobusada, K.; Tsukuda, T. *J. Am. Chem. Soc.* **2005**, *127*, 5261.

(16) Prasad, B. L. V.; Stoeva, S. I.; Sorensen, C. M.; Klabunde, K. J. *Langmuir* **2002**, *18*, 7515.

(17) Ino, S. *J. Phys. Soc. Jpn.* **1969**, *27*, 941.

(18) Marks, L. D. *Philos. Mag. A* **1984**, *49*, 81.

(19) (a) Silly, F.; Castell, M. R. *Appl. Phys. Lett.* **2005**, *87*, 213107. (b) Baletto, F.; Ferrando, R. *Rev. Mod. Phys.* **2005**, *77*, 371.

(20) (a) Hendy, S. C.; Doye, J. P. K. *Phys. Rev. B* **2002**, *66*, 235402. (b) For the estimation, a Mackay icosahedron structure is also assumed. In part a, the total number of atoms in a k -shell Mackay icosahedron is shown to be expressed as $10/3 \cdot k^3 + 5 \cdot k^2 + 11/3 \cdot k + 1$. This gives a sequence of closed-shell Mackay icosahedra with numbers of atoms as follows: 1, 13, 55, ...

(21) Although the face marked with 4 or 5-(1) is slightly inclined with respect to the image plane of FE-SEM, the observed tetragonal arrangements of nanoparticles are not caused by this effect. This was confirmed by the observations of a different superlattice sample from that shown in Figure 5. See the Supporting Information.